Journal of Nuclear Materials 111 & 112 (1982) 39–43
North-Holland Publishing Company

EDGE PLASMA TRANSPORT EXPERIMENTS IN THE CALTECH TOKAMAK

S. ZWEBEN, P.C. LIEWER and R.W. GOULD

Department of Applied Physics, California Institute of Technology, Pasadena, California 91125, USA

This paper describes two experiments on edge plasma transport in the Caltech Research Tokamak ($B_T = 4$ kG, $R = 45$ cm, $a = 15$ cm, $T(\text{edge}) \simeq 25$ eV, $n(\text{edge}) \sim 2 \times 10^{12}$ cm^{-3}). The first aims to understand the mechanism of edge plasma cross-field transport by attempting to measure with Langmuir probes the local $\tilde{E}$ and $\tilde{n}$ and their correlation in order to compute the fluctuation-induced particle flux $\Gamma_{\text{rad}} = c \cdot \langle \tilde{E}_{\text{pol}} \cdot \tilde{n} \rangle / B_T$. The second experiment aims at demonstrating control of the plasma-limiter interaction through use of a local divertor coil mounted inside the limiter itself.

1. Introduction

The plasma-wall interaction in a tokamak is influenced both by atomic physics processes and by plasma processes which transport particles along and across the magnetic field. Both the atomic physics and parallel plasma transport processes are relatively well understood (even though detailed in situ measurements are incomplete), since it is expected that the dominant interactions can be adequately described by simple binary collision cross-sections. However, the cross-field plasma transport coefficients are evidently determined by some sort of plasma turbulence [1] most usually described as "Bohm diffusion" [2]. In fact, there exists very little sure experimental or theoretical ground on which an edge plasma diffusion coefficient $D_\perp$ can be predicted. Thus, models for the scrape-off layer [3] and for heat and particle deposition profiles on the first wall or limiter [4] generally contain $D_\perp$ as an uncertain and uncontrollable parameter.

In section 2 we describe Langmuir probe measurements aimed at determining the $D_\perp$ produced by plasma turbulence in the edge region of the Caltech Research Tokamak ($R = 45$, $a = 15$, $B_T = 4$ kG, $T_{e0} \cong 100$ eV, $n_{e0} \simeq 10^{12}$–10^{13} cm^{-3}). The edge plasma is observed to have $n(\text{edge}) \approx 0.5$–$5 \times 10^{12}$ cm^{-3}, $T_e(\text{edge}) \simeq 25$ eV, along with a large level of broadband density and potential fluctuations, $\tilde{n}/n \simeq e\tilde{\phi}/kT \simeq 10\%$–$50\%$. In an attempt to evaluate the radial particle flux associated with these edge plasma electrostatic fluctuations we measure $\nabla \tilde{\phi}_{\text{pol}}$ with a pair of floating probes and $\tilde{n}$ with a third nearby probe in saturation, thereby allowing a rather direct estimate of the net $\tilde{E} \times B_T$ induced flux.

In section 3 we describe another experiment on edge transport which aims to demonstrate active control of plasma flow to a limiter. Inside the limiter itself is a small coil which makes a type of bundle divertor, the effect of which is to either reduce the plasma density at the side of the limiter by $\times 4$ or increase it by $\times 2$, depending on the direction of the imposed field perturbation. This type of control may be useful in future mechanical pumped-limiter designs.

2. Edge plasma $\tilde{E} \times B$ transport

2.1. Example of $\tilde{n}$ and $\tilde{\phi}$ measurements

In fig. 1(b) is an example of the probe measurements of ion saturation current I^+ and floating potential ϕ_f made using two of the probes of fig. 1(a). In this case the probe tips were both located 1.5 cm past the wall of a limiterless discharge, i.e., at $r/a = 0.9$, and inserted from the outside of the chamber (similar results are obtained when the probe is inserted from the top).

The signals obtained in this way are quite reproducible for similar tokamak discharges, and also change predictably with discharge changes, e.g., I^+ increase at the edge during gas puffing. The magnitude of both ion saturation current I^+ and rms floating potential increase as the probe is moved from 0 to 3 cm in past the wall. However, what remains true at all locations and for all discharge types is that these signals always show large relative fluctuation levels for $r/a \geq 0.8$, i.e.,

$$\tilde{I}^+_{\text{rms}}/I^+ \simeq \frac{e\tilde{\phi}_f}{kT} \simeq 10\%\text{–}50\%.$$

In order to interpret the fluctuations in terms of $\tilde{n}$

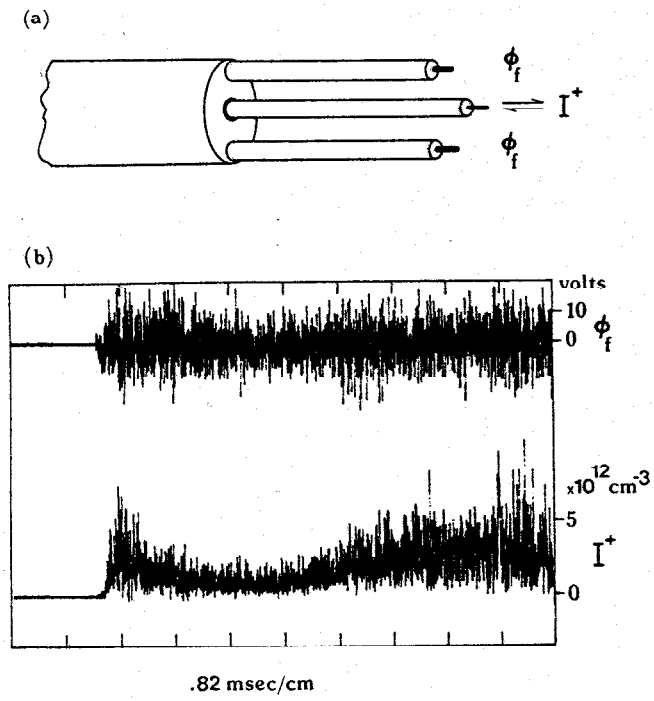

Fig. 1. Langmuir probes as shown in (a) are used in the edge plasma to obtain ϕ_f and I^+, as shown in (b). The mean value of n at $r/a = 0.9$ is approximately $\bar{n}_e/4$ during discharges like this with gas puffing. The probe bias for I^+ is -100 volts here. The Langmuir probe tips are 1 mm × 3 mm tungsten; The shafts are grounded 3 mm diameter stainless.

and $\tilde{\phi}_s$ (space potential), one must in general allow for the possibility that there is also an electron temperature fluctuation $\tilde{T}$ as well as a density and potential fluctuation. If there were a $\tilde{T}$, then the usual simple probe theory would imply a change in I^+ and ϕ_s given by:

$$\left.\begin{aligned} I^+ &\cong \frac{neA}{2}\sqrt{\frac{T_e}{m_i}} \\ \phi_s &= \phi_f + ckT_e \end{aligned}\right\} \qquad (1)$$

where $c \approx 3$. At present we have no measurement of a possible $\tilde{T}$, and since there is some evidence that $\tilde{T}$ is small ($< 5\%$) in other tokamaks [5], we will for the present assume that $\tilde{T} = 0$. Thus we interpret $\tilde{I}^+/I$ as being caused only by $\tilde{n}/n$, and $\tilde{\phi}_f$ to be caused only by $\tilde{\phi}_s$.

2.2. Analysis of $\tilde{n}$ and $\tilde{\phi}_f$

In order to calculate the radial flux we must compute the following quantity:

$$\Gamma = \int \tilde{n}(\omega)\,\tilde{v}_r(\omega)\cos\theta(\omega)\,d\omega, \qquad (2)$$

where $\theta(\omega)$ is the phase angle between $\tilde{n}$ and $\tilde{v}_r$, and $\tilde{v}_r$ is computed assuming $\tilde{v}_r = c\tilde{E}_{pol}/B$. This procedure has been attempted with some success on previous (non-tokamak) experiments [6–8].

We use two floating probes to measure the potential difference $\nabla\tilde{\phi}_f$ (see fig. 1). In order for the result to correctly reflect the local electric field, the probes must be positioned close enough so that they are within a poloidal wavelength and correlation length, but far enough apart so that the probe tips are not shadowing one another; in practice this poloidal probe separation is 0.2–1 cm. The magnitude of $\nabla\tilde{\phi}_f$ vs poloidal separation increases approximately linearly in this range, indicating that the quantity $\tilde{E}_{pol} = \nabla\tilde{\phi}_f/\Delta x_{pol}$ is being measured. Also note that we assume $\tilde{E}_T \ll \tilde{E}_{pol}$ in interpreting the angular rotation of the probe pair as a poloidal probe separation [9].

The density is measured by the I^+ signal from the middle Langmuir probe when this probe is radially aligned with the other two. A check has been made to see that the $\nabla\tilde{\phi}_f$ signal at typically $\Delta x_{pol} = 0.6$ cm has the same magnitude and spectrum with or without the middle probe present, and with or without the middle probe biased to collect either I^+ or I^-.

The analysis of the digitized signals proceeds in a fairly standard way [8,9]. A typical result from one 0.25 ms time-series of $\tilde{n}$ and $\nabla\tilde{\phi}$ data is shown in fig. 2, for a case in which the poloidal probe separation between the two outer probes was 0.6 cm. This data record contains 1024-8 bit samples which were digitized at a 4 MHz sampling rate.

The spectral amplitudes of $\tilde{n}$, $\nabla\tilde{\phi}_f$ and $\tilde{\phi}_f$ itself all have a broadband "turbulent" character, i.e., there are no reproducible or persistent peaks in the spectra and the autocorrelation times are short (≈ 1 μs). The spectral power $P(\omega) \alpha f^{-n}$ has roughly $n \approx 2$ for $f < 200$ kHz and $n \approx 4$ for 300 kHz $< f <$ 1 MHz. In all cases the largest components of $\tilde{n}$ and $\nabla\tilde{\phi}$ are at low frequencies $f \lesssim 200$ kHz, as shown in fig. 2(a), (b). This can be compared to a typical MHD mode frequency typically 20–50 kHz for $m = 2$ for this machine.

The analysis proceeds by calculating the phase and coherence between the two signals, as shown in fig. 2(c) and (d). In order to calculate these quantities a frequency average has been performed over $\Delta f \approx 50$ kHz [9]. One should note that there is only a partial coherence between $\tilde{n}$ and $\nabla\tilde{\phi}$, but that there is enough of a coherence such that the phase between the two is well defined, at least for most of the range below $f \cong 1$ MHz (fig. 2(d)). In this case, at the lowest frequencies the phase between $\tilde{n}$ and $\nabla\tilde{\phi}$ is usually within $0° \pm 60°$, i.e., not that which would be expected between density and electric field in

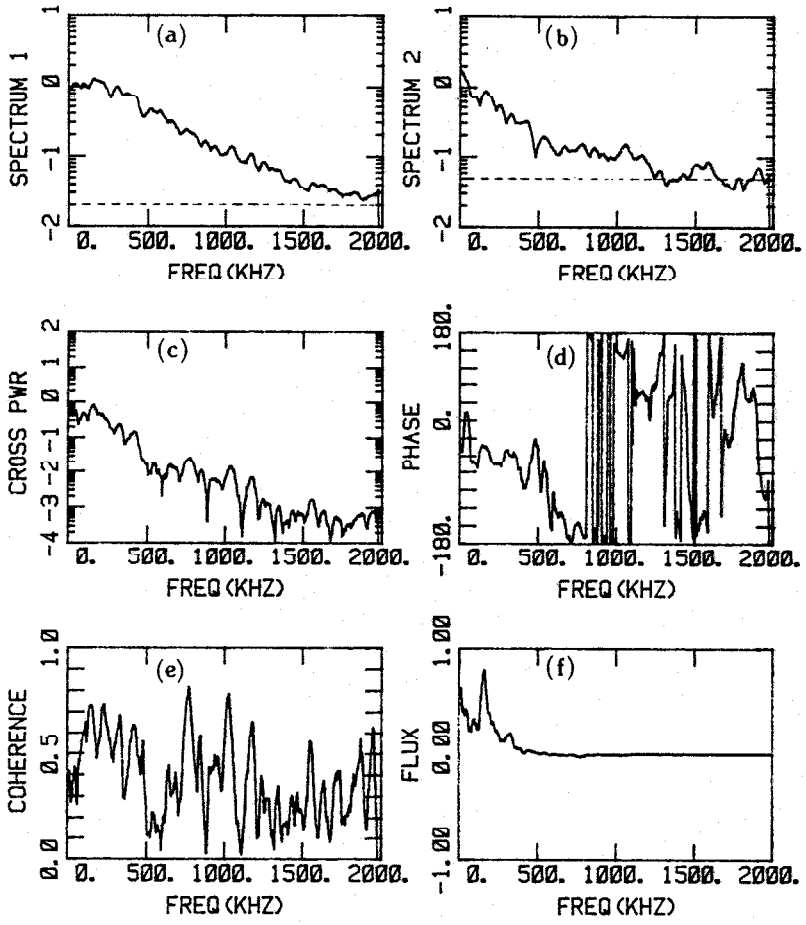

Fig. 2. Analysis of fluctuation spectra includes: (a) amplitude spectrum of $\nabla\tilde{\phi}_f$; (b) amplitude spectrum of $\tilde{n}$; (c) cross-power spectrum of $(\nabla\tilde{\phi}_f, \tilde{n})$; (d) phase between $\nabla\tilde{\phi}_f$ and $\tilde{n}$ (degrees); (e) coherence between $\nabla\tilde{\phi}_f$ and $\tilde{n}$, and (f) radial flux calculated using eq. (2). The system noise levels for the amplitude spectrum are shown by the dashed lines in (a) and (b).

a weakly damped or growing electrostatic wave (i.e., 90°).

The graph in fig. 2(f) is the result of the flux calculation using eq. (1), plotted on a linear vertical scale vs frequency. This is typical of the data obtained so far in this experiment; namely, the largest contribution to the calculated radial flux comes from the low frequency parts of the spectrum at $f < 200$ kHz. The direction for the net flux calculated in this way is radially outward in sign and roughly $\Gamma = 10^{17}$ particles/cm$^2 \cdot$ s.

The experimental results for this section can be summarized as follows: (1) There appear to be large and turbulent density and potential fluctuations in the edge region of our tokamak, with $\tilde{n}/n \approx 0.5$ at $n \simeq 10^{12}$ cm^{-3} and $\tilde{\phi} \approx 10$ V at $T_e \approx 25$ eV; (2) the poloidal electric field $\tilde{E}_{pol}$ measured as $\nabla\tilde{\phi}_f/\Delta x_{pol}$ is $\tilde{E}_{pol} \approx 10$ V/cm, which results in a calculated radial $\tilde{v}_r \simeq 3 \times 10^5$ cm/s: (3) the phase between $\tilde{n}$ and $\tilde{E}_{pol}$ in the low frequency range containing most of the spectral power is within $0° \pm 60°$; and (4) the calculated radial flux is outward and of magnitude $\Gamma \approx \tilde{n}\tilde{v}_r \cos\theta \approx (0.5 \times 10^{12}$ cm$^{-3})$ $(3 \times 10^5$ cm/s$) \cong 10^{17}$ particles/cm$^2 \cdot$ s.

A detailed comparison between this result and the observed particle transport properties of the edge plasma can not yet be made; however, we note the following two points: (a) The outward sign for the flux is reasonable since the neutral penetration length is $\gg 1$ cm, i.e., the ion source is most likely interior to the probe's position; (b) the global particle loss rate as estimated assuming $\tau_p = \tau_E \simeq 1$ ms and axisymmetry is of roughly the same order of magnitude as the result computed from the fluctuations i.e., $\Gamma \sim 10^{17}$ particles/cm$^2 \cdot$ s. This suggests that the observed edge loss rate is dominated by turbulent $\tilde{E} \times B$ diffusion; on the other hand, there are many uncertainties involved in this comparison and this agreement may yet be fortuitous.

3. Local divertor experiments

3.1. Limiter/divertor design

In this section we describe an experiment which demonstrates that the plasma-limiter interaction can be controlled through use of a local magnetic perturbation produced by a coil inside the limiter.

The stainless steel limiter is a box 7.5 cm (vertical) × 5 cm(radial) × 2 cm(toroidal) which is inserted into the plasma edge at the outer equatorial plane. Typically its leading edge can extend up to 4 cm into the chamber ($a = 15$ cm) without seriously degrading the plasma, i.e., at ~ 3 cm insertion the maximum current is reduced from ~ 25 kA without any limiter to ~ 20 kA.

Inside the limiter box is a teflon-insulated 8-turn ~ 4 cm × 6 cm passively cooled copper coil through which a total of up to ~ 20 kA can be passed. The risetime for the current in the coil is ~ 1 ms and the decay time is ~ 20 ms. There is very little mechanical impulse to the limiter structure when this coil is pulsed during the tokamak discharge.

The coil is aligned in the center of the box so that it lies in the plane perpendicular to B_T, such that at the center of the coil its own magnetic field B_c either adds to or subtracts from the normal toroidal field. The magnitude of the B_c at the center of the coil (approximately 2.5 cm from the leading edge of the limiter) can be made equal to or even larger than the normal toroidal field. Thus the local field is significantly perturbed by the coil.

A small, radially movable Langmuir probe is located toroidally adjacent to but outside the limiter box at the equatorial plane in order to measure the local plasma parameters. We report here only on the effect of the field perturbation on the local density as measured by the probe's ion saturation current (the electron saturation current behaves similarly). Thus we assume that the dominant change in I^+ is due to n and not to $\sqrt{T_e}$, which is reasonable since edge temperatures have been observed to be relatively constant in the scrape-off layer [2,4].

3.2. Effects on the edge plasma

Typical results for the effect of the perturbation on the density at the limiter face are shown in fig. 3(a)–(c). In this case the limiter is inserted 3 cm and the probe is positioned 1 cm behind the leading edge of the limiter. When B_c as measured at the center of the coil opposes the normal toroidal field the density at the limiter drops to $\lesssim 1/4$ of its unperturbed value. When the perturbed field direction is switched the density increases to $\gtrsim 2$ times its unperturbed value. For smaller values of B_c the density change varies roughly linearly with perturbed field.

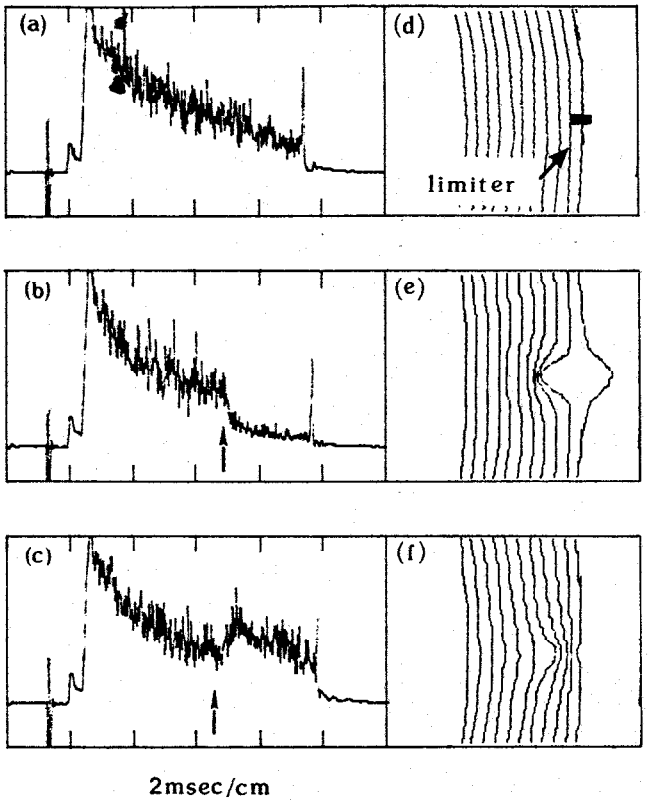

Fig. 3. Effect of limiter coil perturbation on I^+ at limiter face: (a) $B_c = 0$; (b) $B_c \cong -B_T$; (c) $B_c \cong +B_T$. The arrows show when limiter coil is energized (risetime $\simeq 1$ ms). Computer plots of toroidal field lines (top view) for these cases are shown in (d)–(f); the limiter location is shown in (d).

This qualitative behavior is quite consistent and reproducible for various plasma and limiter conditions, i.e., for limiter insertions of 2.5–4 cm and for the full range of edge plasma density on this machine. The radial profile of the density change shows the greatest effect for the case shown in fig. 3 (~ 1 cm behind the limiter's leading edge), but similar changes occur throughout the scrape-off layer including the leading edge region. There is little change of the bulk plasma due to these edge perturbations, except for a slow increase in impurity levels after the limiter density is increased at the coil.

We can only mention here a few points which will enter into full analysis of the experiment: (1) The dominant cause of the observed changes seems to be the expansion or contraction of the flux tube as it ap-

proaches the limiter face. In fig. 3(d)–(f) are shown computer plots of the expected toroidal field lines for the cases of fig. 3(a)–(c) respectively; (2) the perturbation also moves field linear radially as in a bundle divertor [10], thus changing the boundary conditions for cross-field transport. It is not yet clear how the scrape-off layer thickness in the limiter shadow (normally 1–2 cm) is affected by the perturbations; (3) effects of the perturbation on the edge plasma potential, temperature, or fluctuation level are also possible. So far it appears that the perturbation coil changes mainly the edge density profile, and that the other plasma parameters remain approximately constant. In particular we should note, in connection with section 2 of this paper, that the density and potential fluctuations in the limiter shadow appear quite similar to those observed at the edge of limiterless discharges, as was also observed on Macrotor [9].

4. Conclusion

We have shown that: (a) the tokamak edge plasma has a large electrostatic fluctuation level which most likely produces the observed Bohm-type edge particle transport, and (b) the plasma-limiter interaction can be easily controlled by a local bundle-type divertor. Further experiments along the lines of section 2 need to be done in order to check for $\tilde{T}$ and for possibly non-axisymmetric particle fluxes. Also, more reactor relevant (large area) geometries are needed to check the operation of devices like that in section 3.

Acknowledgement

We thank R. Fowler, V. Lynch and J. Rome of ORNL for the use of their tokamak magnetic field line code. This work was performed under the DOE contract (DE-AS03-76SF00767).

References

[1] J.D. Callen et al., 8th Intern. Conf. on Plasma Physics and Cont. Nuclear Fusion Research, Brussels, 1980, Paper #IAEA-CN-38/Y-3; P.J. Harbour and G. Proudfoot, Proc. IAEA Technical Committee Meeting on Divertors and Impurity Control, Garching, 1981, paper I.C9; C.M. Surko and R.E. Slusher, Phys. Fluids 23 (1980) 2425; E. Mazzucato, Phys. Fluids 21 (1978) 1063.

[2] Y. Gomay et al., Nucl. Fusion 18 (1978) 849; S.J. Zweben and R.J. Taylor, UCLA Report PPG-543 (1981), submitted to Nucl. Fus..

[3] J.M. Ogden et al., IEEE Trans. Plasma Sci., UPS-9, #4 (1981) p. 274.

[4] R.W. Conn (ed.), Fusion Engineering Device, Vol. IV Sec. 4, DOE/TIC-1160 (1981).

[5] G.F. Tait, F.J. Stauffer and D.A. Boyd, Phys. Fluids 24 (1981) 719.

[6] P. Broissier, Nucl. Fusion 18 (1978) 867.

[7] H.W. Hendel, T.K. Chu and P.A. Politzer, Phys. Fluids 11 (1968) 2426.

[8] J.R. Roth et al., J. Appl. Phys. 52 (1981) 2075.

[9] S.J. Zweben and R.J. Taylor, Nucl. Fusion 21 (1981) 193.

[10] P.E. Stott, C.M. Wilson, A. Gibson, Nucl. Fusion 18 (1978) 475.